

**REMOVAL OF COBALT FROM SULPHATE
SOLUTIONS USING AN ELECTROGENERATIVE
PROCESS**

by

TAN WAN XIN

**Thesis submitted in fulfillment of the
requirements for the degree of
Master of Science**

June 2011

ACKNOWLEDGEMENT

I would like to acknowledge and extend my heartfelt gratitude to the following persons who have made the completion of this thesis possible:

- Prof. Norita Mohamed for the guidance and encouragement throughout my study.
- Dr. Hamzah Darus, for the invaluable knowledge and ideas he shared.
- Mr. Ariffin, Mr. Marimuthu, Mr. Ali, Mrs. Saripah and Mrs. Norhayati and fellow lab assistants as well as staff in the School of Chemical Sciences for their constant assistance and help throughout my research work.
- Ms. Jamilah and Mr. Johari from School of Biological Sciences for help with SEM analysis.
- Mr. Kharuna from School of Physics for help with XRD analysis.
- Ministry of Science, Technology and Innovation, for postgraduate research scholarship.
- Lab members and friends in the School of Chemical Sciences for their support and friendship.
- Especially to my family and friends, for their understanding, encouragement and unconditional support.

TABLE OF CONTENTS

	Page
Acknowledgement	ii
Table of contents	iii
List of tables	vii
List of figures	viii
List of symbols	xi
List of abbreviations	xiii
Abstrak	xiv
Abstract	xvi
CHAPTER 1 INTRODUCTION	1
1.1 Background of Cobalt	1
1.2 Health Concerns	2
1.3 Application of Cobalt in Industries	3
1.4 Treatment Technologies	5
1.4.1 Ion Exchange	5
1.4.2 Precipitation	6
1.4.3 Cementation	6
1.4.4 Adsorption	7
1.4.5 Electrodialysis	8
1.4.6 Electrochemical Processes	9
1.4.6.1 Electrogenative Process	9
1.4.6.1.1 Electrogenative Removal of Cobalt from Sulphate Solutions	11

1.5	Objectives of Research	12
CHAPTER 2 REVIEW OF COBALT REMOVAL FROM SULPHATE SOLUTIONS		15
2.1	The Chemistry of Cobalt Reduction with the Influence of pH	15
2.2	Types of Reactor	18
2.3	Reactor Configuration	20
2.4	Choice of Electrode Materials	20
	2.4.1 Porous Graphite	20
	2.4.2 Reticulated Vitreous Carbon (RVC)	22
2.5	Mass Transport Characteristics and Reactor Design Equations	26
CHAPTER 3 EXPERIMENTAL		30
3.1	Cobalt Removal with Batch Reactor	30
	3.1.1 Materials and apparatus	30
	3.1.2 Experimental Procedure	34
	3.1.2.1 Treatment of Cathodes	34
	3.1.2.2 Preparation of Electrolytes	34
	3.1.2.3 Cathodic Polarization Studies	34
	3.1.2.4 Electrogenerative Cobalt Removal Using a Batch Reactor	35
3.2	Cobalt Removal with Batch-recycle Reactor	35
	3.2.1 Materials and apparatus	38
	3.2.2 Experimental Procedure	38
	3.2.2.1 Treatment of Cathodes	38

3.2.2.2	Preparation of Electrolytes	38
3.3.2.3	Electrogenerative Cobalt Removal Using a Flow-by Batch-recycle Reactor	39
3.3	Determination of Kinematic Viscosity of Co(II) solutions	42
3.4	Voltammetric Studies	42
3.5	Analysis	43
3.5.1	Atomic Absorption Spectroscopy (AAS)	43
3.5.2	Scanning Electron Microscopy-Energy Dispersive X-ray Analysis (SEM-EDX)	43
3.5.3	X-ray Diffraction (XRD)	43
3.6	Experimental Approach	43
CHAPTER 4 RESULTS AND DISCUSSION: BATCH REACTOR		46
4.1	Polarization Studies	46
4.2	Effect of pH on Cobalt Removal	49
4.3	Effect of Different Cathode Materials	54
4.4	Effect of Initial Cobalt(II) Ion Concentration	55
4.5	Effect of Na ₂ SO ₄ Concentration	57
4.6	SEM, EDX and XRD Analyses	57
CHAPTER 5 RESULTS AND DISCUSSION: BATCH-RECYCLE REACTOR		63
5.1	Determination of Kinematic Viscosity	64
5.2	Determination of Diffusion Coefficient	64
5.3	Effect of pH on Cobalt Removal	66
5.4	SEM, EDX and XRD analyses	70
5.5	Effect of Initial Co(II) Ion Concentration	75

5.6	Effect of Electrode Porosity	79
5.7	Mass Transport Correlations	84
CHAPTER 6 CONCLUSIONS AND FUTURE WORK		87
6.1	Conclusions	87
6.2	Recommendations for Future Work	88
REFERENCES		89
APPENDICES		
Appendix A Properties of Porous graphite and RVC		
Appendix B Properties of Anion Exchange Membrane		
Appendix C Experimental Results		
Appendix D List of publications		

LIST OF TABLES

Table		Page
2.1	Review of mass transport correlation for system using RVC electrodes.	29
3.1	Details of experimental conditions for batch reactor.	36
3.2	Details of experimental condition for batch-recycle reactor.	41
4.1	Polarization characteristics for 80 ppi RVC and PG-25 as cathodes at different pH in 200 mg L ⁻¹ cobalt sulphate solution.	48
4.2	Cell performance for the cobalt recovery from 200 mg L ⁻¹ cobalt sulphate medium at different pH on 80 ppi RVC and PG-25 cathodes.	53
5.1	Experimental time recorded and the calculated kinematic viscosities of different concentrations of cobalt sulphate solution.	65
5.2	Cell performance for cobalt removal using 100 ppi RVC from different initial Co(II) concentration with varying of electrolyte flow rates.	78
5.3	Values of $k_m A_e$ and k_m calculated from the slopes of inset plots of Figs. 5.9 to 5.11 and the percent of cobalt removal after 4 h of experiment.	83

LIST OF FIGURES

Figure	Page
1.1 Cobalt demand patterns in terms of end-use products (1995 vs. 2005).	4
1.2 Charge transfer and ion transport in an electrogenerative reactor with an anion exchange membrane.	13
2.1 Pourbaix diagram for Cobalt-H ₂ O system.	17
2.2 Schematic diagrams of (a) batch reactor, (b) continuous stirred tank reactor, and (c) plug flow reactor.	19
2.3 Reactor configuration: (a) flow-through, and (b) flow-by.	21
2.4 Structure of porous graphite.	23
2.5 SEM micrograph that shows the honeycomb structure of RVC.	24
3.1 Experimental setup and electrical circuit for a batch reactor.	31
3.2 The ionic selectivity principal of an anion exchange membrane.	33
3.3 Schematic diagram of the flow-by reactor.	37
3.4 Experimental set-up and hydraulic flow circuit of batch-recycle reactor system.	40
3.5 Outline of experimental approach.	44
4.1 Cathodic polarization curves for systems utilizing 80 ppi RVC and PG-25 as cathodes with 200 mg L ⁻¹ cobalt(II) in 0.1 M Na ₂ SO ₄ and 0.4 M H ₃ BO ₃ at different pH values. (◆) pH 4.0, RVC; (■) pH 3.5, RVC; (▲) pH 3.0, RVC; (×) pH 4.0, PG-25; (□) pH 3.5, PG-25; (Δ) pH 3.0, PG-25.	47
4.2 Percent of removal vs. time with RVC and PG-25 as cathodes at different pH values from 200 mg L ⁻¹ cobalt(II) in 0.1 M Na ₂ SO ₄ and 0.4 M H ₃ BO ₃ . (◆) pH 4.0, RVC; (■) pH 3.5, RVC; (▲) pH 3.0, RVC; (◇) pH 4.0, PG-25; (□) pH 3.5, PG-25; (Δ) pH 3.0, PG-25. Error bars displayed are standard error of percentage of cobalt removal for three replicates.	50
4.3 Linearization of normalized concentration of cobalt as a function of time with RVC and PG-25 cathodes at different pH values from 200 mg L ⁻¹ cobalt(II) in 0.1 M Na ₂ SO ₄ and 0.4 M H ₃ BO ₃ . (◆) pH 4.0, RVC; (□) pH 4.0, PG-25; (Δ) pH 3.5, PG-25.	52

4.4	Percent of removal vs. time at different initial Co(II) concentration at pH 4.0 on 80 ppi RVC cathode in 0.1 M Na ₂ SO ₄ and 0.4 M H ₃ BO ₃ . (◆) 10 mg L ⁻¹ ; (□) 200 mg L ⁻¹ ; (Δ) 500 mg L ⁻¹ . Error bars displayed are standard error of percentage of cobalt removal for three replicates.	56
4.5	Percent of removal vs. time at different Na ₂ SO ₄ concentrations at pH 4.0 on 80 ppi RVC cathode from 200 mg L ⁻¹ cobalt(II) in 0.4 M H ₃ BO ₃ . (◆) 0 M Na ₂ SO ₄ ; (■) 0.1 M Na ₂ SO ₄ ; (▲) 0.2 M Na ₂ SO ₄ . Error bars displayed are standard error of percentage of cobalt removal for three replicates.	58
4.6	SEM micrograph of cobalt deposits on 80 ppi RVC at pH 4.0. (a) magnification of 1000 x (b) magnification of 3000 x.	59
4.7	EDX analysis of cobalt deposits on 80 ppi RVC at pH 4.0 at magnification of 50 x.	60
4.8	XRD analysis of cobalt deposits on 80 ppi RVC at pH 4.0.	62
5.1	Variation of cathodic peak current vs. scan rate of cobalt on different RVC electrodes. (●) 60 ppi RVC; (■) 80 ppi RVC; (▲) 100 ppi RVC.	67
5.2	Percent of removal vs. time with 100 ppi RVC from 500 mg L ⁻¹ Co(II) at pH 4.00. (●), 50 mL min ⁻¹ ; (□), 100 mL min ⁻¹ ; (Δ), 150 mL min ⁻¹ ; (◆), 200 mL min ⁻¹ . Error bars displayed are standard error of percentage of cobalt removal for three replicates.	69
5.3	Percent of removal vs. time with 100 ppi RVC from 500 mg L ⁻¹ Co(II) at condition of no pH adjustment. (●), 50 mL min ⁻¹ ; (□), 100 mL min ⁻¹ ; (Δ), 150 mL min ⁻¹ ; (◆), 200 mL min ⁻¹ . Error bars displayed are standard error of percentage of cobalt removal for three replicates.	71
5.4	SEM micrograph of cobalt deposits on 100 ppi RVC at condition of no pH controlled. (a) magnification of 500 x (b) magnification of 3000 x.	72
5.5	EDX analysis of cobalt deposits on 100 ppi RVC with no pH controlled at magnification of 100 x.	73
5.6	XRD analysis of cobalt deposits on 100 ppi RVC with no pH controlled.	74
5.7	Percent of removal vs. time from 10 mg L ⁻¹ Co(II) with 100 ppi RVC. (●), 50 mL min ⁻¹ ; (□), 100 mL min ⁻¹ ; (Δ), 150 mL min ⁻¹ ; (◆), 200 mL min ⁻¹ . Error bars displayed are standard error of percentage of cobalt removal for three replicates.	76

5.8	Percent of removal vs. time from 100 mg L ⁻¹ Co(II) with 100 ppi RVC. (●), 50 mL min ⁻¹ ; (□), 100 mL min ⁻¹ ; (Δ), 150 mL min ⁻¹ ; (◆), 200 mL min ⁻¹ . Error bars displayed are standard error of percentage of cobalt removal for three replicates.	77
5.9	Normalized concentration [C_t/C_o] vs. time from 100 mg L ⁻¹ Co(II) with 60 ppi RVC. Inset: Plots of ln [C_t/C_o] vs. time for the data shown. (●), 50 mL min ⁻¹ ; (□), 100 mL min ⁻¹ ; (Δ), 150 mL min ⁻¹ ; (◆), 200 mL min ⁻¹ .	80
5.10	Normalized concentration [C_t/C_o] vs. time from 100 mg L ⁻¹ Co(II) with 80 ppi RVC. Inset: Plots of ln [C_t/C_o] vs. time for the data shown. (●), 50 mL min ⁻¹ ; (□), 100 mL min ⁻¹ ; (Δ), 150 mL min ⁻¹ ; (◆), 200 mL min ⁻¹ .	81
5.11	Normalized concentration [C_t/C_o] vs. time from 100 mg L ⁻¹ Co(II) with 100 ppi RVC. Inset: Plots of ln [C_t/C_o] vs. time for the data shown. (●), 50 mL min ⁻¹ ; (□), 100 mL min ⁻¹ ; (Δ), 150 mL min ⁻¹ ; (◆), 200 mL min ⁻¹ .	82
5.12	Double logarithmic plots of specific mass transport coefficient, $k_m A_e$ vs. linear flow velocity, u for cobalt removal from 100 mg L ⁻¹ Co(II) with different RVC grades. (●), 60 ppi RVC; (○), 80 ppi RVC; (◆), 100 ppi RVC.	85

LIST OF SYMBOLS

a	empirical constant
\AA	angstrom, nm
A_e	specific surface area, m^{-1}
A_x	cross-sectional area of electrode, m^2
B	empirical constant
θ	angle of incidence
λ	wavelength
i_p	peak current, A
C_t	metal concentration at time t , mol m^{-3}
C_o	initial metal concentration, mol m^{-3}
C	concentration of analyte, mol m^{-3}
D	diffusion coefficient, $\text{m}^2 \text{s}^{-1}$
E	voidage of porous electrode
E°	standard reduction potential, V
E°_{cell}	overall cell potential, V
F	empirical constant
F	Faraday's constant, C mol^{-1}
ΔG°	standard Gibb's free energy, J mol^{-1}
k_m	mass transport coefficient, m s^{-1}
K	viscometer constant
m	empirical constant
n	empirical constant
n	number of electrons

θ	angle of incidence
Q	volumetric flow, $\text{m}^3 \text{s}^{-1}$
R	correlation coefficient
R	universal gas constant, $\text{J K}^{-1} \text{mol}^{-1}$
Re	Reynolds number
Sc	Schmidt number
Sh	Sherwood number
t	time, s
T	absolute temperature, K
u	electrolyte velocity, m s^{-1}
v	scan rate of the potential, V s^{-1}
ν	kinematic viscosity, $\text{m}^2 \text{s}^{-1}$
V_e	cathode volume, m^3
V_R	volume of electrolyte, m^3
y	kinetic energy correction, s

LIST OF ABBREVIATIONS

2D	two-dimensional
3D	three-dimensional
AAS	atomic absorption spectrometer
BR	batch reactor
CDI	cobalt development institute
CSTR	continuously stirred tank reactor
DMT	dimethyl terephthalate
EDX	energy dispersive X-ray
GBC	gas diffusion electrode packed bed electrode cell
HER	hydrogen evolution reaction
PFR	plug flow reactor
ppi	pores per inch
PG-25	porous graphite
PET	polyethylene terephthalate
PTA	terephthalic acid
RCE	rotating cylinder electrode
RVC	reticulated vitreous carbon
SEM	scanning electron microscopy
SCE	saturated calomel electrode
XRD	X-ray diffraction

PENYINGKIRAN KOBALT DARIPADA LARUTAN SULFAT MENGUNAKAN PROSES ELEKTROGENERATIF

ABSTRAK

Suatu sistem elektrogeneratif digunakan untuk menyingkirkan kobalt dari larutan sulfat. Dalam proses ini, suatu tindak balas kimia berlaku secara spontan dalam sel yang dibahagikan di mana penurunan kobalt berlaku pada katod dan zink dioksidakan pada anod tanpa bekalan tenaga dari luar. Dalam kajian ini, dua jenis mod operasi (reaktor berkelompok dan reaktor berkelompok kitar-semula) telah dikaji.

Sistem elektrogeneratif untuk menyingkirkan kobalt telah digunakan dalam sebuah reaktor berkelompok yang telah dilengkapi dengan elektrod tiga-dimensi: 80 liang per inci (ppi) karbon kaca berongga (RVC) dan grafit berliang (PG-25) sebagai bahan katod. Keputusan yang diperolehi menunjukkan bahawa 80 ppi RVC berfungsi sebagai bahan katod yang lebih sesuai daripada PG-25 dalam sistem ini. Pada keadaan optimum, lebih daripada 99% kobalt telah disingkirkan dan diperolehi dalam keadaan logam selepas beroperasi selama 10 jam dengan kepekatan awal larutan kobalt sebanyak 200 mg L^{-1} pada pH 4.0 dalam $0.2 \text{ M Na}_2\text{SO}_4$ dan $0.4 \text{ M H}_3\text{BO}_3$.

Suatu reaktor aliran-tegak lurus yang beroperasi dalam mod kitar semula berkelompok telah diperkembangkan. RVC digunakan sebagai bahan katod. Kajian penurunan Co(II) pada 100 ppi RVC telah dijalankan dengan menggunakan kepekatan awal Co(II) sebanyak 500 mg L^{-1} dengan kawalan pH 4.00 pada kadar alir elektrolit 50, 100 150 dan 200 mL min^{-1} . Penyingkiran kobalt yang tidak memuaskan

iaitu kurang daripada 75% telah diperolehi pada semua kadar alir elektrolit selepas beroperasi selama 8 jam. Dalam eksperimen lain, larutan uji yang sama telah digunakan tetapi tanpa kawalan pH sepanjang eksperimen ($\text{pH awal} = 5.44 \pm 0.10$). Masa yang lebih pendek telah dicatat iaitu 7 jam digunakan untuk menyingkirkan lebih daripada 99% kobalt pada semua kadar alir. Dengan itu, keadaan pH tersebut telah dipilih untuk kajian seterusnya. Penggunaan 60 ppi RVC dalam reaktor menghasilkan nilai k_m yang paling tinggi jika dibandingkan dengan gred RVC yang lain. Nilai k_m didapati menurun dengan meningkatnya keliangan katod pada keadaan eksperimen yang digunakan..

REMOVAL OF COBALT FROM SULPHATE SOLUTIONS USING AN ELECTROGENERATIVE PROCESS

ABSTRACT

An electrogenerative system is applied to removing cobalt from sulphate solutions. In this process, a chemical reaction takes place spontaneously in a divided cell where cobalt is reduced at the cathode and zinc is oxidised at the anode without an external supply of energy. In this work, two types of operating modes (batch reactor and batch-recycle reactor) were investigated.

The electrogenerative removal of cobalt is conducted in a batch reactor equipped with three-dimensional electrodes: 80 pores per inch (ppi) reticulated vitreous carbon (RVC) and porous graphite (PG-25) as cathode materials. Results obtained show that 80 ppi RVC serves as a more suitable cathode material than PG-25 in this system. At optimum conditions, more than 99% of cobalt was removed and recovered in its metallic state after 10 h of operation with an initial 200 mg L^{-1} Co(II) solution at pH 4.0 in $0.2 \text{ M Na}_2\text{SO}_4$ and $0.4 \text{ M H}_3\text{BO}_3$.

A flow-by reactor operated in a batch recirculation mode was also developed. RVC was used as the cathode material. Studies of Co(II) reduction on 100 ppi RVC were accomplished using 500 mg L^{-1} Co(II) concentration at pH 4.00 and with electrolyte flow rates of 50, 100, 150 and 200 mL min^{-1} . It was shown that poor removal of < 75% cobalt was achieved at all flow rates after 8 h of operation. In another set of experiments, without pH adjustment throughout the experiments (initial pH = 5.44 ± 0.10), similar test solutions were used. It was noteworthy that a shorter time of 7 h was required to remove more than 99% of cobalt at all flow rates.

Therefore, further studies were done without pH adjustment. The use of 60 ppi RVC in the reactor resulted in the highest k_m value compared to other grades of RVC. k_m value was found to decrease with increasing cathode porosity under the experimental condition used.

CHAPTER 1

INTRODUCTION

1.1 Background of Cobalt

Cobalt, together with nickel and iron, are defined as the iron-group metals. It is a hard and lustrous metal which is silverish or grayish-white in colour. As reported by the Cobalt Development Institute (CDI) and tabulated by Kapusta (2006), progressive growth of cobalt production had occurred from a total production of 23,207 tonnes in 1995 to 53,635 tonnes in 2005. This more than twofold increase was in conjunction with the increasing demand of cobalt in various industries. Based on the available sources, CDI predicted that the total world cobalt production could be about 80,030 tonnes in 2010, mainly due to the anticipated growth in demand for batteries, superalloys, magnets, etc (Kapusta, 2006).

Cobalt prices have been relatively unstable over the years. In 2003, the price of high grade cobalt was only about USD16 kg⁻¹. Following that, there was a sharp increase in price to about USD50 and USD40 kg⁻¹ in 2004 and 2005 respectively (Jandová *et al.*, 2005; Marafi and Stanislaus, 2008). In early 2008, the average London Metal Bulletin price for high grade cobalt reached USD86 kg⁻¹. However, a dramatic fall in price was noted in October 2008 when the price declined to about USD29 kg⁻¹. Apparently, this drastic fall in price coincided with the collapse in the global economy. In September 2009, after the worst of the global recession had passed, the price for high grade cobalt increased to about USD44 kg⁻¹ (The Cobalt Development Institute, 2009).

Pure cobalt does not exist naturally in metallic state. It is commonly found as ores form in combination with sulphides, either nickel or copper oxides/ sulphides or occasionally cobalt arsenides. Small amounts of it are generally extracted as by-products in the mining and processing of nickel and copper ores. It was reported that considerable amounts of cobalt may also be found in silver, gold, lead and zinc ores; however, their processing does not always lead to cobalt recovery (Jandová *et al.*, 2005; The Cobalt Development Institute, 2006a). Due to the scarce production of cobalt, it being least abundant compared to nickel and copper and the high consumption of cobalt in industries, recycling or treatment of cobalt from industrial wastes are deemed important.

1.2 Health Concerns

Cobalt is a non-biodegradable heavy metal and tends to accumulate in the environment. The effluents containing cobalt if discharged without treatment will pose a serious health hazard to humans and contribute to environmental pollution. Prolonged exposure to cobalt has given rise to many diseases and disorders in humans. Among them are dermatitis, lung affection, with symptoms of cough and shortness of breath, pneumoconiosis, and gastric disturbance with symptoms included vomiting, severe pain and tenderness in the epigastrium as well as pain in the limbs with marked weakness. Carcinogenic and mutagenic effects of Co in rats have also been verified due to acute cobalt poisoning (Browning, 1969; Venugopal and Luckey, 1978; Elinder and Friberg, 1979; Vincoli, 1997). As a result of its high toxicity, the removal of cobalt from industrial effluents is of major concern. In Malaysia, it was unexpected that there are still no finite rules for the permissible level of cobalt in wastewater. However, in other countries, like Lithuania, the

permissible concentration of cobalt(II) in the sewage effluents is restricted to 500 ug L⁻¹ (Snukiškis and Kaušpediene, 2005). It was also reported that the maximum limits of cobalt in irrigation water and livestock watering are 500 and 1000 µg L⁻¹ respectively (Nagpal *et al.*, 2006).

1.3 Application of Cobalt in Industries

Cobalt is prevalent and widely used in many industries. Today, most of the world's cobalt is used predominantly to produce superalloys (Ni/Co/Fe), batteries, hard materials (carbides), magnets, catalysts and so on. From 1995 to 2005, there has been a significant shift in worldwide cobalt demand patterns in terms of end-use products, as summarized in Fig. 1.1. A high demand of cobalt in rechargeable batteries (lithium ion batteries) has been observed in recent years mainly due to the extensive use of such batteries as electrochemical power sources in mobile phones, personal computers and other portable electronic devices (Nan *et al.*, 2005; Swain *et al.*, 2007). Cast cobalt-base superalloys are widely used in military and commercial aircraft turbine engines for vanes and other high temperature structural components (Jiang *et al.*, 1999).

Cobalt is also deployed in the manufacture of various magnetic materials. The remarkable use of samarium-cobalt magnets was developed in the early 1970s. They are the second strongest type of magnets beside neodymium magnets. Cobalt-based magnets are commonly used to overcome the thermal instability and poor corrosion resistance which are usually found in other types of magnetic materials (The Cobalt Development Institute, 2009). There has been a slight increase in the application of cobalt as catalysts owing to its multivalent characteristics (Co²⁺ and

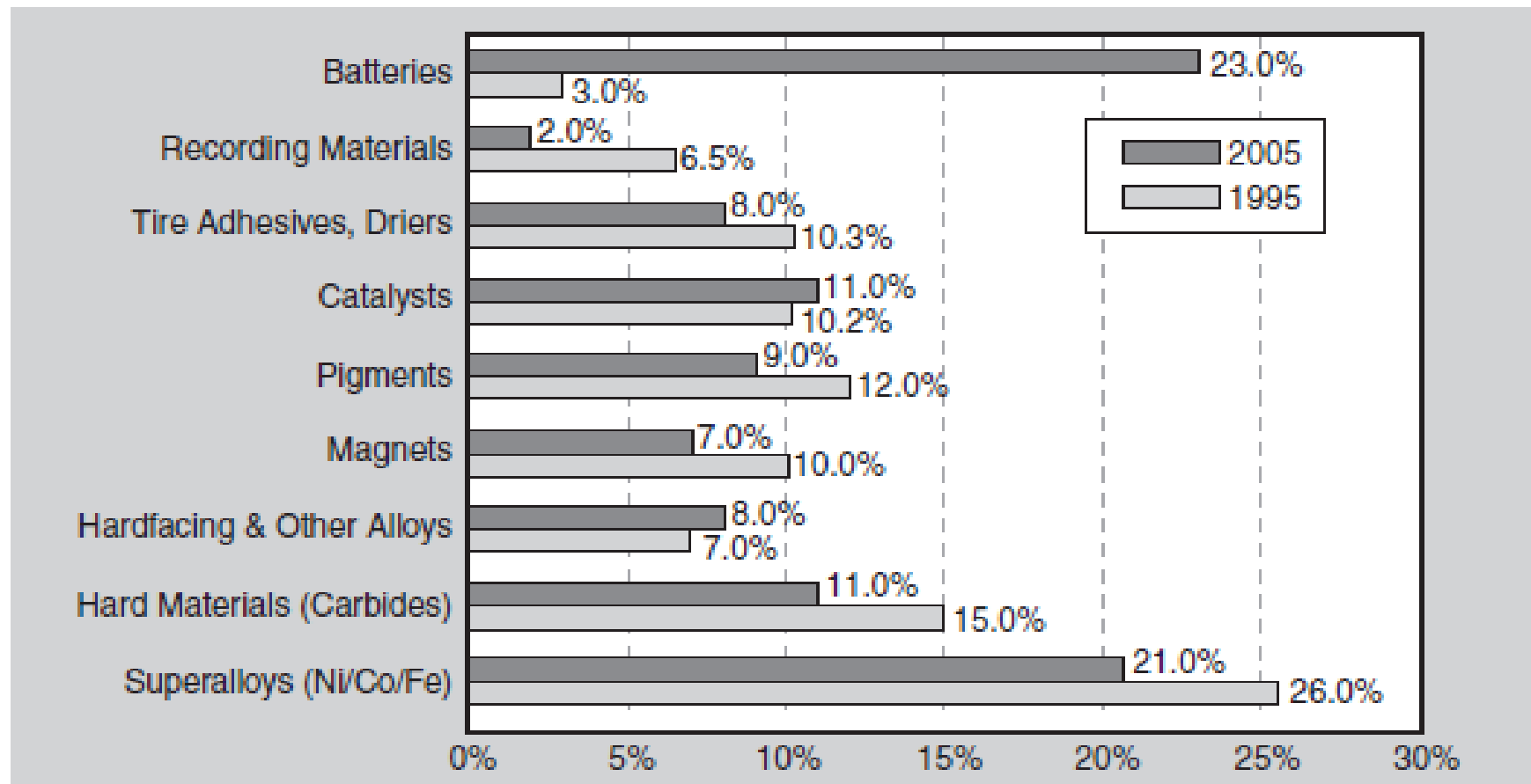


Figure 1.1 Cobalt demand patterns in terms of end-use products (1995 vs. 2005) (adapted from Kapusta, 2006).

Co³⁺). It is used in the production of terephthalic acid (PTA) and dimethyl terephthalate (DMT) for the manufacture of polyethylene terephthalate (PET) used to produce polyester fibres and synthetic textiles for packaging, PET bottles and recording tapes. Cobalt-molybdenum-alumina catalysts are also used in the hydrodesulphurization of petroleum (The Cobalt Development Institute, 2006b; Wang, 2006).

1.4 Treatment Technologies

The rapid growth of industries has resulted in the generation of large amounts of effluents that contain heavy metals. Heavy metals are non-biodegradable, toxic and carcinogenic agents. The release of heavy metals into the environment has become of great concern in recent years due to their hazardous effects. The concentration of metal ions in effluent solutions is normally $< 1000 \text{ mg L}^{-1}$ (Walsh, 2001). Laws and acts had been proposed to restrict and reduce the concentration of heavy metals to below their permissible levels before being discharged into the environment. In view of these issues, various treatment technologies have been utilised to remove and recover metal ions from process solutions. These are discussed at length as follows:

1.4.1 Ion Exchange

Ion exchange involves an interchange of ions between two electrolytes or between an electrolyte solution and a solid phase (Qureshi and Varshney, 1991). In most cases the term is used to denote the processes of purification, separation, and decontamination of aqueous and other ion-containing solutions with solid polymeric or mineralic ion exchangers. Ion exchangers are either cation exchangers that

exchange positively charged ions (cations) or anion exchangers that exchange negatively charged ions (anions). There are also amphoteric exchangers that are able to exchange both cations and anions simultaneously. Cobalt had been removed by ion exchange using a chelating resin (Mendes and Martins, 2004). However, this method is often too costly and suitable ion exchangers are not available for all metal ions (Jüttner *et al.*, 2000).

1.4.2 Precipitation

Precipitation involves removal of a dissolved metal (cationic form) from solution. The cations are converted to an insoluble form (particle) by a chemical reaction between the soluble metal compounds and the precipitating reagent (Szabadvary, 1992). The particles formed by this reaction are removed from solution by settling or filtration. Removal of cobalt through the precipitation process has been carried out by Huang *et al.* (2004) and Oustadakis *et al.* (2006). The precipitation process has economical limitations and the effectiveness of this process is dependent on several factors, including the type and concentration of ionic metals present in solution, the precipitant used, the reaction conditions (especially the pH of the solution), and the presence of other constituents that may inhibit the precipitation reaction. The major drawback of this process is the generation of secondary pollutants due to the sludge that remains after treatment (Njau *et al.*, 1998; Lanza and Bertazzoli, 2000; Gasparotto *et al.*, 2006).

1.4.3 Cementation

Cementation is the simplest and oldest hydrometallurgical process (Cao and Duby, 2001). It involves the reaction wherein a more noble metal is reduced from the

electrolyte onto a less noble metal, which will oxidise and replace it in the solution. During cementation, cobalt is usually reduced from the solutions by zinc dust or powder (van der Pas and Dreisinger, 1996; Dreher *et al.*, 2001; Boyanov *et al.*, 2004). The overall cementation reaction is simplified as (Bøckman and Østvold, 2000):



The kinetics of the cementation process is generally influenced by two types of behavior. In the first type, the cementation rate is initially slow followed by an enhanced rate (faster rate). This is maybe due to the increase of surface area by deposits, the separation of zero concentration and zero velocity planes near the precipitant metal surface or the formation of eddy diffusion at the boundary layer by the deposit protrusions. In the second type, the cementation rate decreases with time due to the formation of the smooth deposits which results in the difficult diffusion of ions through this layer (Chaudhury and Bhattacharya, 1989).

1.4.4 Adsorption

Adsorption is the adhesion of a chemical species onto the surface of particles as opposed to absorption in which the molecules actually enter the absorbing medium. Adsorption occurs when interaction between an adsorptive and an adsorbent resulting in a particular arrangement of an adsorbate on the surface (Selim and Iskandar, 1999). Krishnan and Anirudhan (2008) and Sulaymon *et al.* (2009) had dealt with adsorption of cobalt on activated carbon. However, this adsorbent has gradually lost its popularity due to its relative high capital and regeneration cost

(Ahmadpour *et al.*, 2009; Bhatnagar *et al.*, 2010). Low cost adsorbents such as almond green hull (Ahmadpour *et al.*, 2009), lemon peel (Bhatnagar *et al.*, 2010), sepiolite (Kara *et al.*, 2003) and fungal-based biosorbents, PFB1 (Suhasini *et al.*, 1999) and kaolinite (Yavuz *et al.*, 2003) have been investigated as a replacement for activated carbon.

1.4.5 Electrodialysis

Electrodialysis is a membrane separation process during which ions are selectively transported through an ion-exchange membrane under the influence of an electric field. For a three compartments reactor, the cell consists of cathodic, anodic and centre compartments. A cation exchange membrane is placed between the cathodic and centre compartments and an anion exchange membrane is installed between the anodic and centre compartments. This arrangement of membranes allowed ions to be passed through one membrane and blocked by the next. When a current is applied to the system, anions and cations will migrate in accordance with their charges forming two main streams, viz. diluate and concentrate compartments. Anions migrate toward the anode and cations migrate toward the cathode crossing the anion and cation exchange membranes respectively. Electrodialysis has inherent weakness where it is less efficient in removing non-charged, higher molecular weight and less mobile ionic species. The fouling of an ion exchange membrane due to clogging would reduce the efficiency of the electrodialysis system (Janssen and Koene, 2002). This system had been applied by Chaudhary *et al.* (2000), Nelson *et al.* (2000), Tzanetakis *et al.* (2003), Marder *et al.* (2004) and Pazos *et al.* (2010).

1.4.6 Electrochemical Processes

Electrochemical processes cover both electrolytic and galvanic processes. The processes are of a heterogeneous nature as the reactions are taking place at the interface of the electrode and the electrolyte (Juttner *et al.*, 1999). Electrochemical processes involve redox reactions where an electron is transferred to or from a molecule or ion by changing its oxidation state. This reaction can occur through the application of an external voltage or through the release of chemical energy. Electrolytic removal of metal had been studied by most authors. The electrolytic removal of lead had been studied by Ponce de Leon and Pletcher (1996), Widner *et al.* (1998) and Gasparotto *et al.* (2006). Pradhan *et al.* (2001) and Sharma *et al.* (2005) had conducted electrowinning of cobalt from sulphate solutions, while Mishra *et al.* (2002) had carried out electro-reduction of cobalt. However, the electrolytic process is not cost effective when dealing with very dilute solutions with low metal ion concentrations as parasitic reactions would take place, reducing the current and removal efficiency (Almeida *et al.*, 2008). In order to achieve high recoveries, high electrical power input is required which would subsequently increase operating costs. Therefore, in order to reduce the operating cost while removing metal ions at the same time, an electrogenerative process (galvanic process) is introduced as an alternative to the electrolytic process.

1.4.6.1 Electrogenative Process

The use of an electrogenerative process which is a galvanic process, for the removal and recovery of cobalt is introduced as an alternative to the electrolytic process. From the thermodynamics view, the Gibb's free energy change, ΔG^0 is negative for a spontaneous reaction system. Thus, for an electrogenerative process

(Rajeshwar and Ibanez, 1997):

$$\Delta G^0 = -nFE_{\text{cell}}^0 \quad (1.2)$$

where n is the number of electrons accepted or released by the reaction per mole of reagent, F is Faraday's constant, E_{cell}^0 is the overall cell potential. In the electrogenerative process, a chemical reaction takes place spontaneously in a divided cell where a more noble metal is reduced at the cathode and a less noble metal is oxidised to produce electrical energy without an external supply of energy. The roles of these metals as oxidising and reducing agents are determined by referring to their reduction electrode potentials. The metal ions with more electropositive reduction potentials tend to undergo reduction.

The electrogenerative system had been demonstrated to successfully remove and recover metal ions from process solutions. Njau and Janssen (1998) carried out the reduction of chromate from a very low concentration of 20 mg L^{-1} in a gas diffusion electrode packed bed electrode cell (GBC). A final concentration of chromate $< 0.5 \text{ mg L}^{-1}$ was achieved. The reactor combined the catalytic oxidation of hydrogen gas in the gas diffusion electrode and the simultaneous reduction of chromate ions on the porous cathode without the need of an external power source. Chieng (2005) studied the reduction of hexavalent chromium to trivalent chromium using electrogenerative flow reactors with different configurations; flow-through or flow-by modes. Results showed that both reactors could reduce an initial chromate concentration of 10 mg L^{-1} to below 0.05 mg L^{-1} at electrolyte flow rates of 5 mL min^{-1} .

The electrogenerative removal and recovery of copper from rinse electroplating rinse solutions had been carried out by Hor and Mohamed (2003, 2005) using a flow-by reactor operated in single-pass and batch-recycle modes. The batch-recycle system proved to be more suitable than the single-pass system in treating low copper wastewater. The system operating at 500 mL min^{-1} successfully removed an initial copper(II) concentration of 74.2 mg L^{-1} to $< 1.0 \text{ mg L}^{-1}$ after 150 min.

Yap and Mohamed (2007, 2008a) studied gold recovery from cyanide solutions using a batch reactor and a batch-recycle reactor. With the batch reactor system, more than 99% of gold could be recovered from an initial gold concentration of 500 mg L^{-1} within 1 h using an activated reticulated vitreous carbon (RVC) as cathode material. For the batch-recycle system, the flow-through reactor proved to be efficient in treating low Au(I) concentrations. At an initial Au(I) concentration of 10 mg L^{-1} , more than 95% of gold can be recovered within 3 h of operation at all electrolyte flow rates.

1.4.6.1.1 Electrogenerative Removal of Cobalt from Sulphate Solutions

The electrogenerative removal and recovery of cobalt will be carried out with a batch reactor and a flow-by reactor. Three dimensional porous electrodes will be used as cathode materials with zinc as an anode. The anion exchange membrane in the reactor allows charge transfer through the electrolytes but prevents mixing of the electrolytes between the cathode and anode compartments. The cathode is placed in the catholyte compartment and the zinc anode is placed in the anolyte compartment. When the cell is short circuited, zinc metal with a lower reduction potential than

cobalt will be oxidized and at the same time cobalt ions will be reduced at the cathode. The flow of electrons from the Zn terminal to the Co half-cell is shown in Fig. 1.2. The galvanic reaction can be represented by the following equations:



E^0 values given in Eqs. 1.3 and 1.4 are standard reduction potential values for the reduction half-reactions. From the overall positive potential of the cell (in Eq. 1.5) and the free Gibbs energy (in Eq. 1.2), the reaction should have favourable thermodynamics to be able to occur spontaneously without an external supply of energy.

1.5 Objectives of research

This work represents the pioneering efforts on cobalt removal which has been conducted via an electrogenerative process. In this work, the use of an electrogenerative process which is a galvanic process is introduced as an alternative treatment technology for the removal and recovery of cobalt from sulphate solutions. The electrogenerative system is applied in removing cobalt from dilute solutions. Two types of operating modes (batch reactor and batch-recycle reactor) were investigated. The performance of the batch reactor system was evaluated with different parameters, viz. types of electrode materials used, initial cobalt(II) concentration, cathode potential, influence of pH and concentration of sodium

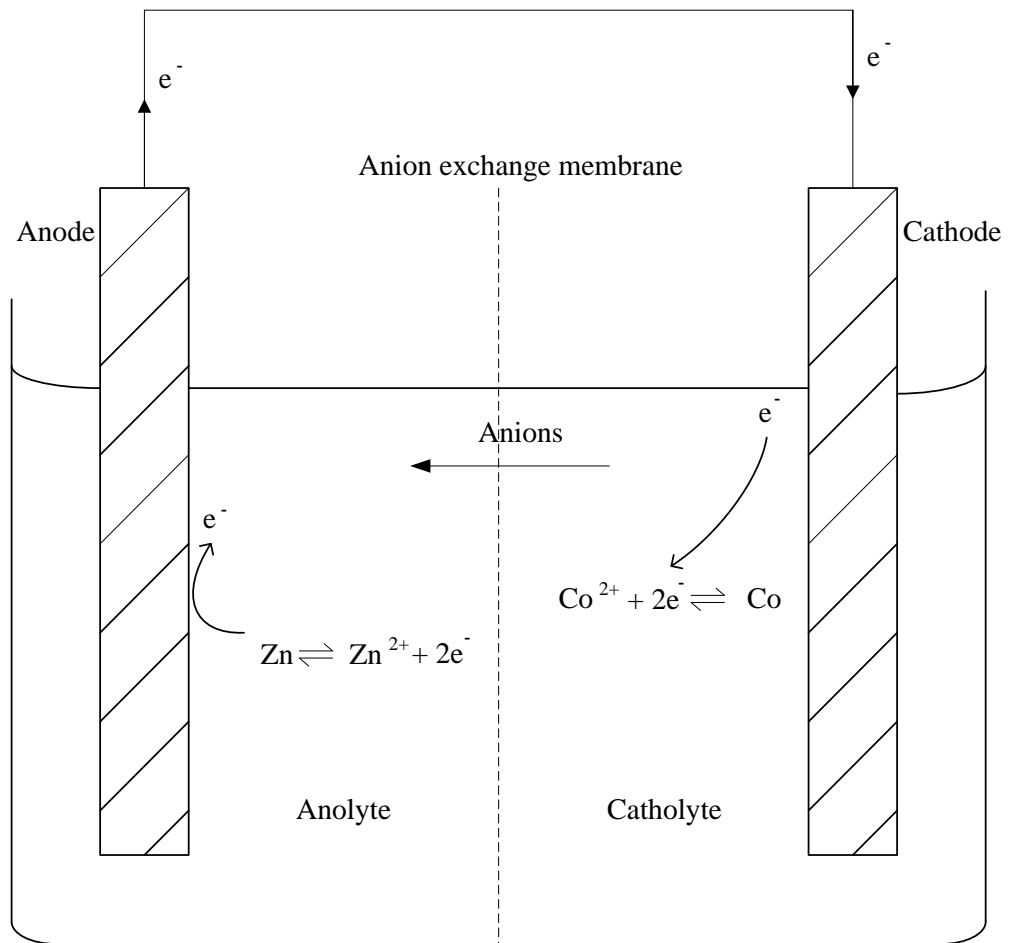


Figure 1.2 Charge transfer and ion transport in an electrogenerative reactor with an anion exchange membrane.

sulphate as supporting electrolyte. Optimum conditions for the removal and recovery of cobalt with particular cobalt(II) concentration were also investigated.

Investigations were carried out to find the suitable pH conditions for cobalt removal using a batch-recycle reactor. The most appropriate pH condition was then selected for further studies. The performance of the system was further evaluated with varying electrolyte flow rates, initial Co(II) concentration and cathode porosity. The mass transport characteristics of the system with different cathode porosities were also determined.

CHAPTER 2

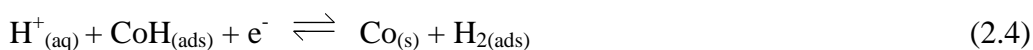
REVIEW OF COBALT REMOVAL FROM SULPHATE SOLUTIONS

2.1 The Chemistry of Cobalt Reduction with the Influence of pH

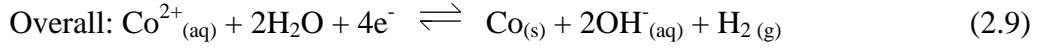
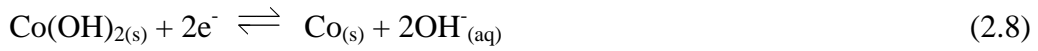
The influence of pH on the electrodeposition mechanisms of cobalt has been discussed by some authors (Matsushima *et al.*, 2006; Garcia *et al.*, 2008). It was proposed that cobalt deposition is always influenced by two different pathways of hydrogen evolution reaction (HER); (Eqs. 2.3–2.4) and (Eqs. 2.6–2.8), which depend on pH. Theoretically, the main cathodic reactions which are likely to occur in the cathodic compartment are (Sharma *et al.*, 2005):



However, it is proposed that for $\text{pH} < 4.0$, cobalt deposition goes through an adsorbed intermediate, CoH which will be subsequently reduced to metallic cobalt (Eqs. 2.7-2.8) (Garcia *et al.*, 2008).

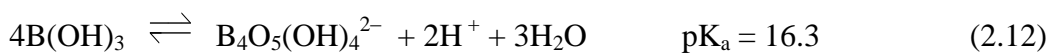
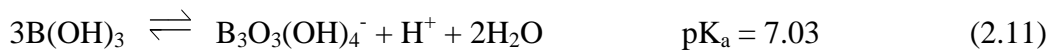


For $\text{pH} > 4.0$, water reduction (Eq. 2.6) leads to an increase of pH in the vicinity of the cathode surface. This can result in the precipitation of cobalt hydroxide, which is then reduced to metallic cobalt (Eqs. 2.7-2.8).



At $\text{pH} > 4.0$, Garcia *et al.* (2008) reported that anomalous co-deposition occurred when the pH at the electrode surface was lower than that required for the formation of $\text{Co}(\text{OH})_2$ (at $\text{pH} > 8.5$) as shown in the Pourbaix diagram (Fig. 2.1) for the cobalt- H_2O system. This was due to a substantial increase in pH in the vicinity of the electrode surface caused by water reduction.

To counteract the abrupt increase of pH and the formation of $\text{Co}(\text{OH})_2$, boric acid is added in the bath solution. Boric acid acts as a buffer to retard water reduction (Ji and Cooper, 1996; Zech and Landolt, 2000; Santos *et al.*, 2007). At low concentrations, boric acid reacts with water to form the mono-borate ion, while at higher boric acid concentrations (greater than 0.1 M) mostly tri- and tetra-borates are formed (Zech and Landolt, 2000). The following are the reactions to be considered in the presence of boric acid:



The dissociation reaction produces additional protons in the catholyte compartment, hence preventing an abrupt increase in pH . Furthermore, addition of boric acid

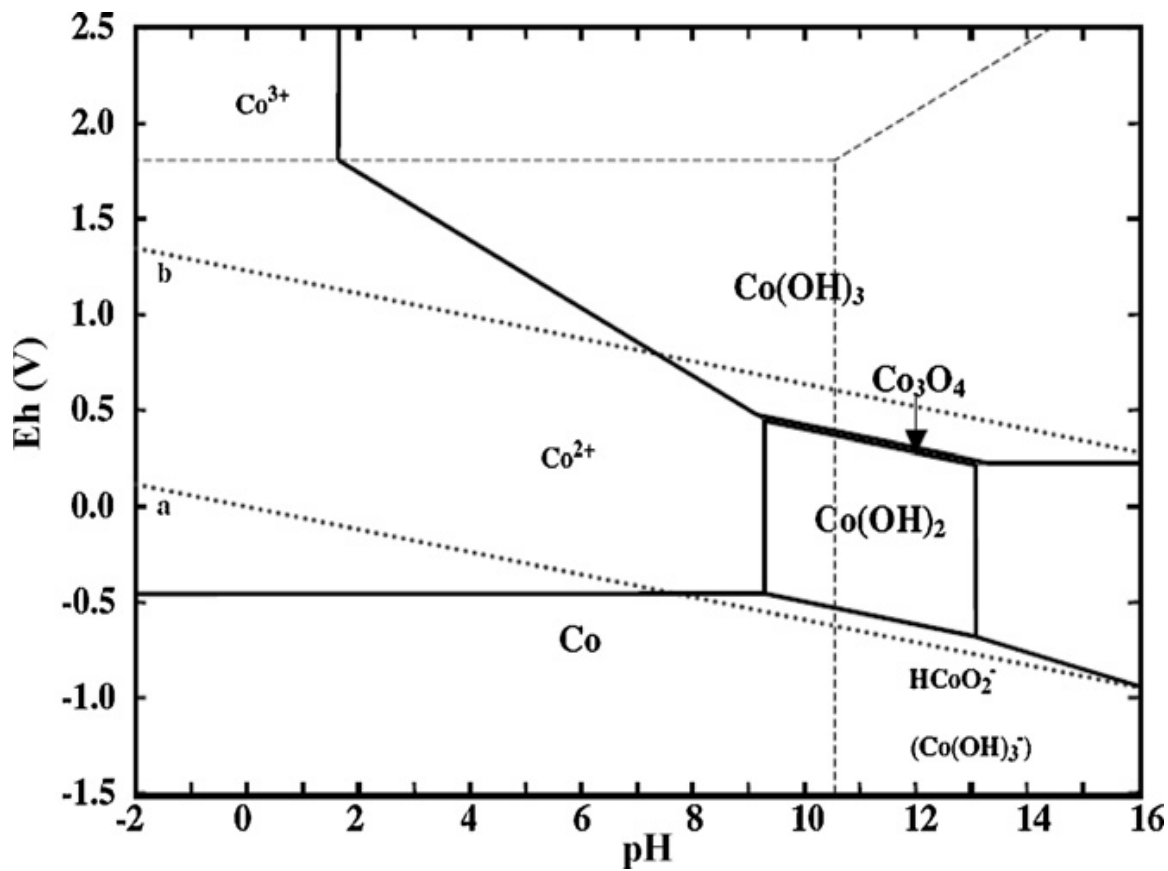


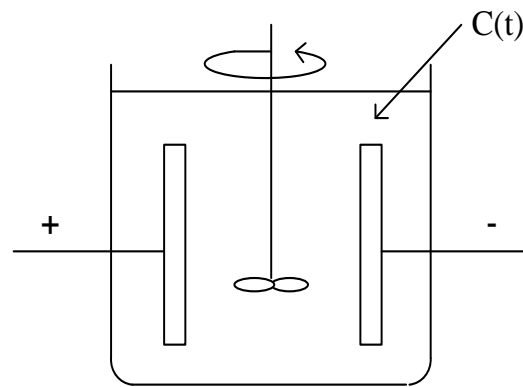
Figure 2.1 Pourbaix diagram for Cobalt-H₂O system (adapted from Garcia *et al.*, 2008).

enhances the appearance of deposits which are brighter and less brittle (Zech and Landolt, 2000; Tripathy *et al.*, 2001).

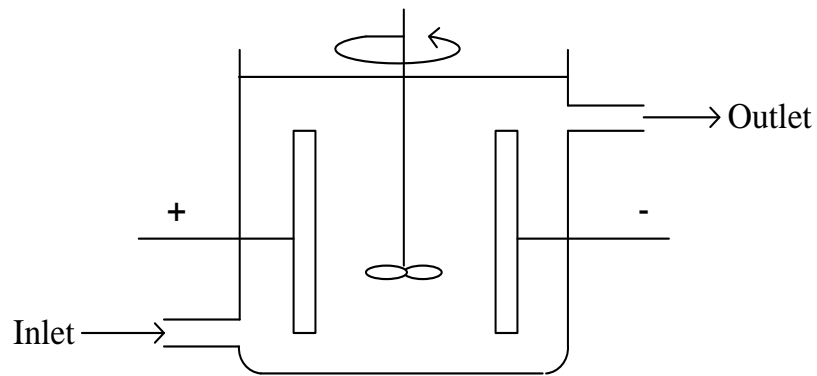
2.2 Types of Reactor

There are generally three types of reactors; namely batch reactor (BR), continuous stirred tank reactor (CSTR) and plug flow reactor (PFR) (Pletcher and Walsh, 1993; Trinidad *et al.*, 1998). Schematic diagrams of the three reactor types are depicted in Fig. 2.2. Among the reactors, BR is commonly used for small-scale operations due to its simplicity, versatility and economically. In the batch reactor, the reactant is continuously stirred as a function of time during which reaction occurs to some extent. It is a time-dependent system, where the concentration of reactants and products will progressively change with time but the composition is uniform throughout the reactor volume. In Fig. 2.2a, $C(t)$ is the concentration of reactants after time, t . CSTR consists of a perfectly stirred tank reactor with a continuous flow of electrolyte through it. Therefore, the concentration of reactants and products are uniform throughout the reactor. For the case of CSTR, the reactant concentration within the reactor is equal to that at the outlet and is independent of time. For PFR, the electrolyte flows continuously through the reactor with no mixing of the electrolyte with that preceding or following it. The reactants and products will change with distance through the reactor but they are independent of time. Therefore, the residence time is the same for all species. In Chapter 4, BR will be used to investigate the removal of cobalt from sulphate solutions. This system with a recirculation mode; namely as a batch-recycle reactor, will be further explored in Chapter 5.

(a)



(b)



(c)

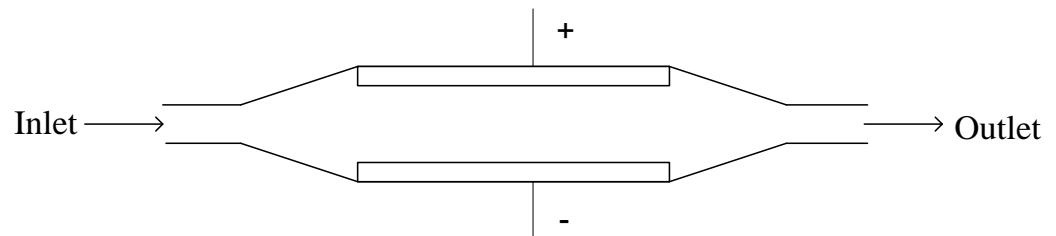


Figure 2.2 Schematic diagrams of (a) batch reactor, (b) continuous stirred tank reactor, and (c) plug flow reactor (adapted from Trinidad *et al.*, 1998).

2.3 Reactor Configuration

For the batch-recycle system, the flow reactor can be basically designed into two different configurations; flow-through or flow-by modes (Pletcher and Walsh, 1992). In the flow-through configuration or also known as axial-field flow, the direction of the electrolyte flow is parallel to the electrical current flow. These directions are perpendicular to each other when the flow-by configuration (radial-field flow) is employed (Ferreira, 2008). Fig. 2.3 illustrates the flow-through and flow-by configurations with respect to the directions of current and electrolyte flow.

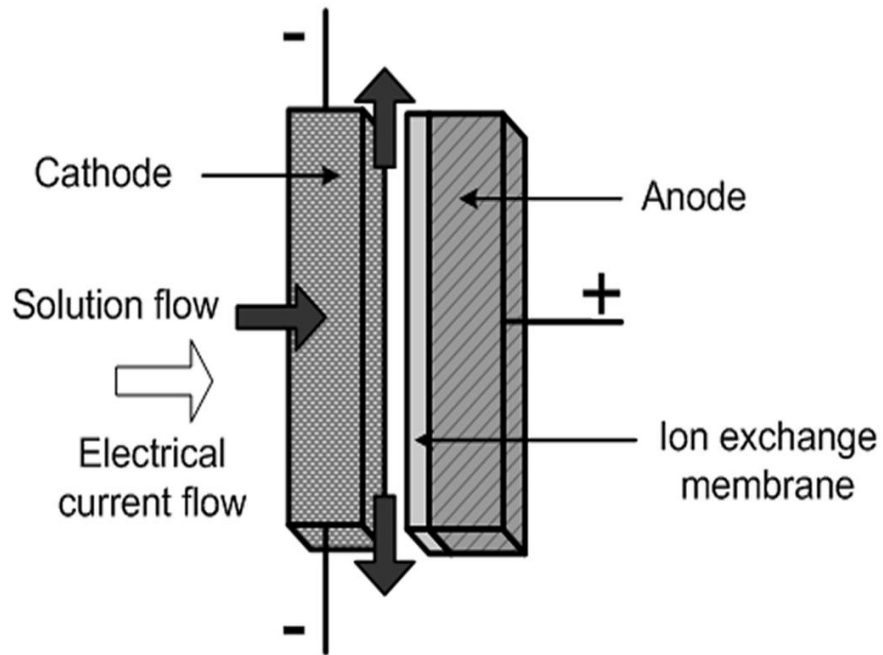
2.4 Choice of Electrode Materials

The electrodes which are equipped in the electrochemical reactors can be classified into two groups: two-dimensional (2D) electrodes and three-dimensional (3D) electrodes. These electrodes can be used under static as well as moving conditions. 3D electrodes are more superior to 2D electrodes. These are owing to their inherent properties; the electrodes are distributed throughout all three dimensions in contrast to the planar configuration. This arrangement can counteract the limitations of low specific surface areas and low space-time yield (Jüttner *et al.*, 2000). Examples of 3D electrodes include porous graphite, carbon felt, reticulated vitreous carbon (RVC), packed bed electrodes and fluidized bed electrodes. Among these 3D electrodes, porous graphite and RVC are chosen as cathode materials and their performances and effects on cobalt removal will be compared in Chapter 4.

2.4.1 Porous Graphite

Apart from diamond, graphite is one of the best known allotropes of carbon. It is formed from a series of stacked parallel layer planes, where all the layer planes

(a)



(b)

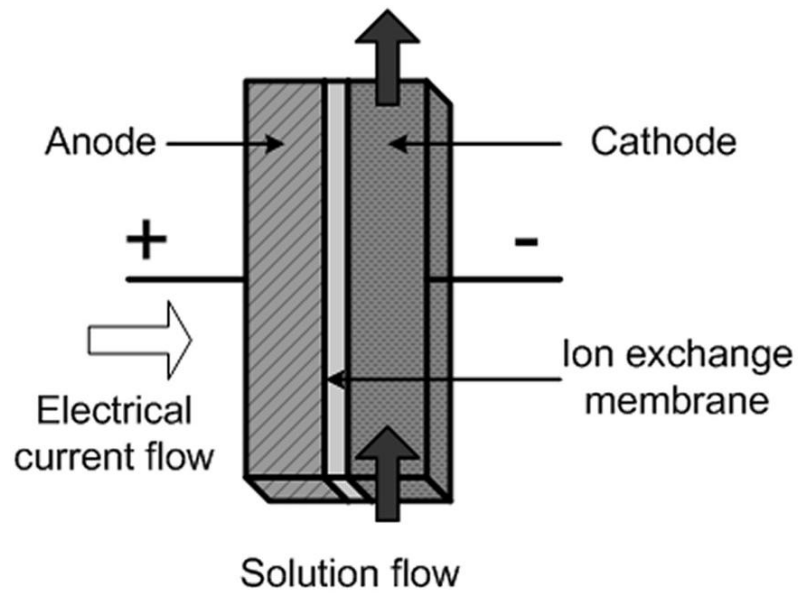


Figure 2.3 Reactor configuration: (a) flow-through, and (b) flow-by (adapted from Yap and Mohamed, 2008b).

are built up with the trigonal sp^2 bonding. Within each layer plane, the carbon atom is covalently bonded to three other carbon atoms, forming a series of hexagonal rings as depicted at Fig. 2.4. The layer planes are mostly positioned in the hexagonal structure, with a stacking sequence, ABABAB. Another structure of graphite is the rhombohedral form with the layer sequence, ABCABCABC. It is always found in combination with hexagonal graphite and occurs in small amounts in some natural and synthetic graphite. Unlike diamond, graphite is able to conduct electricity due to the delocalization of the pi bond electrons above and below the planes of carbon atoms. The hybridized fourth valence electron is paired with another delocalized electron of the adjacent plane by the weak van der Waals forces. These electrons are free to move along the plane of the layers (Pierson, 1993).

2.4.2 Reticulated Vitreous Carbon (RVC)

RVC is a form of glass-like carbon which has some properties of glass and some properties of the normal industrial used carbons (Energy Res. Gen. Inc., 2009). It is an open-pore foam material of honeycomb structure formed by strands of carbon (struts). The distinct structure of RVC (from scanning electron microscopy (SEM) image) is shown in Fig. 2.5. It has several available pore size grades ranging from 10 to 100 pores per inch (ppi). It is selected as a cathode material in this study due to its properties of exceptional large void volume, large surface area, high porosity, chemical inertness, resistance to very high temperature, and good electrical conductivity (Friedrich *et al.*, 2003). The drawbacks of RVC include brittleness and less resistance to high mechanical loads.

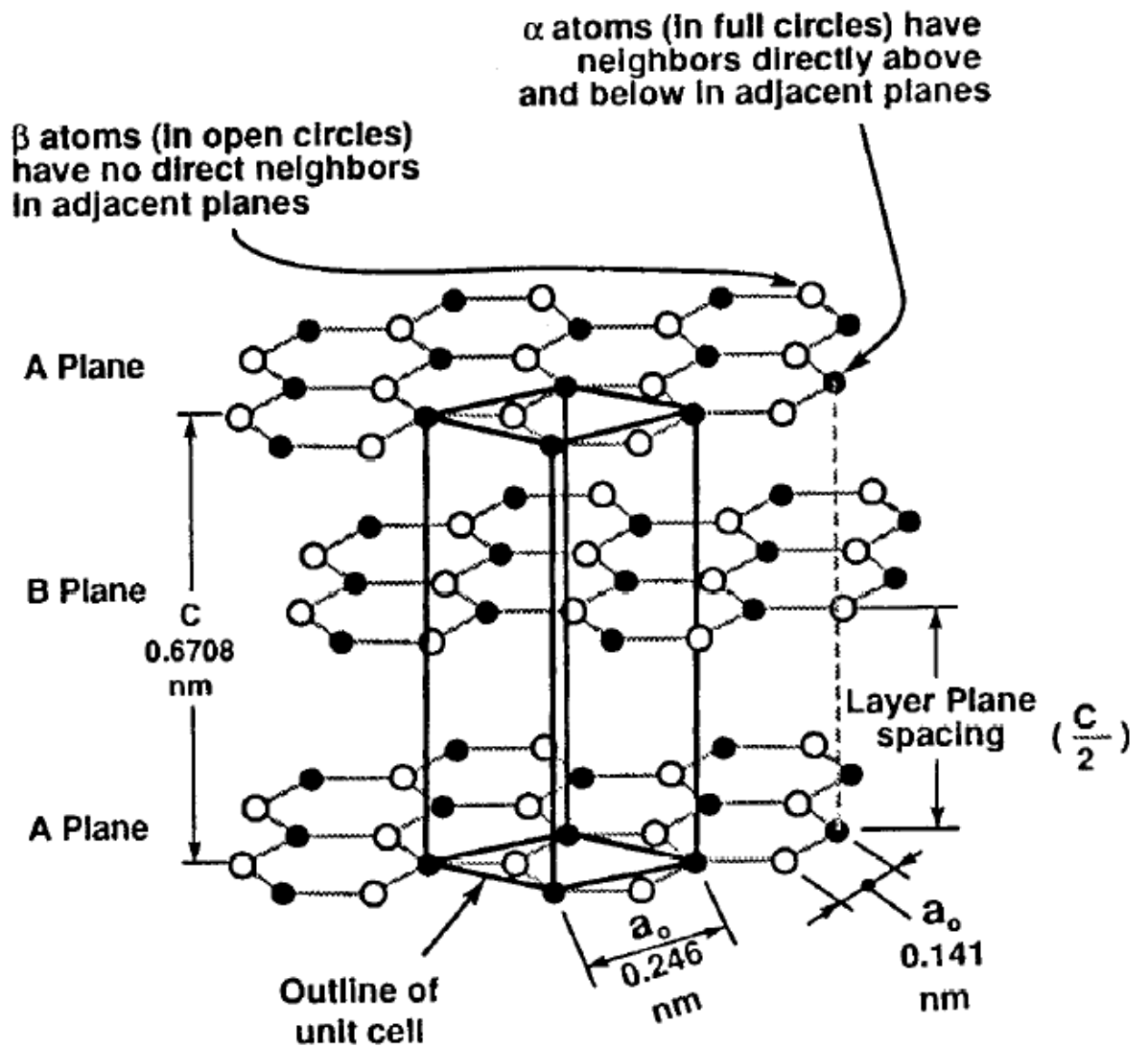


Figure 2.4 Structure of porous graphite (Source: Pierson, 1993).

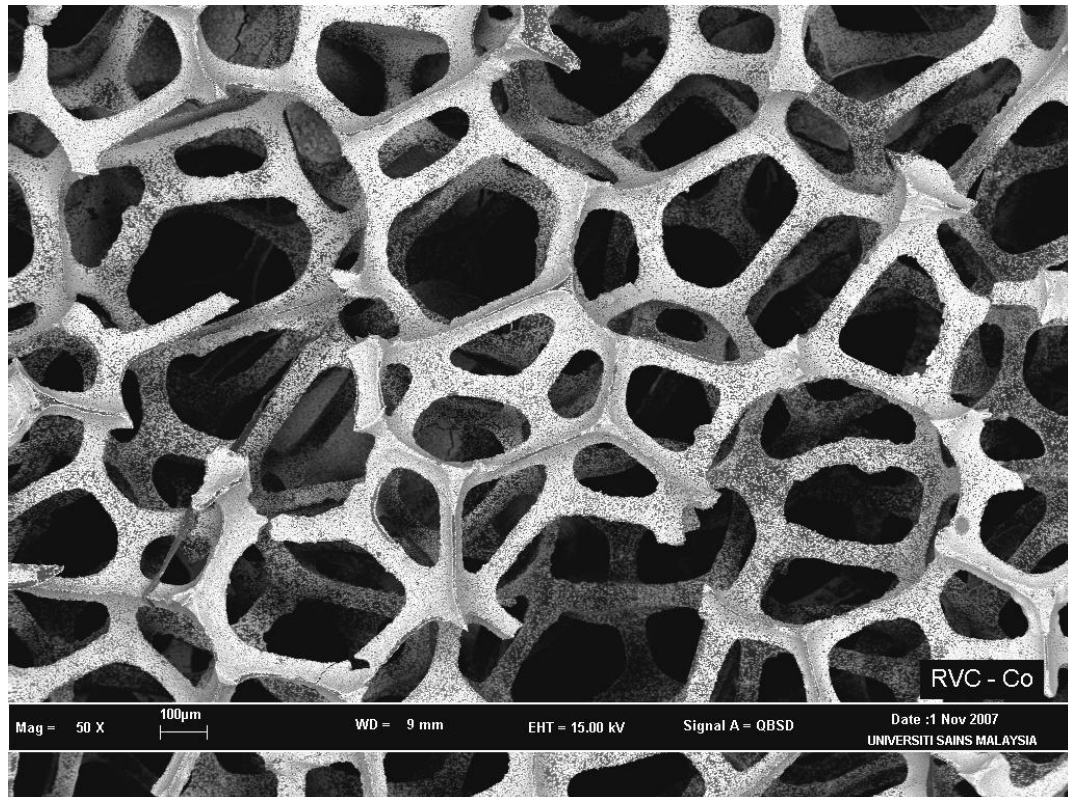


Figure 2.5 SEM micrograph that shows the honeycomb structure of RVC.

RVC has been extensively used over the past decades for studies on metal ion removal (Friedrich *et al.*, 2003). Reade *et al.* (2004a) employed RVC rotating cylinder electrodes (RCE) of different porosities (10, 30, 60 and 100 ppi) to study the removal of cupric ions from acidic sulphate solutions. It was reported that the rate of concentration decay increased corresponding to the porosity grades. The fastest rate of copper removal to concentration $< 0.1 \text{ mg L}^{-1}$ was achieved using a 100 ppi RVC. Reade *et al.* (2004b) had also worked on cadmium removal from sulphate solutions, selective removal of copper followed by cadmium removal from sulphate solutions and copper removal from chloride medium using 100 ppi RVC RCE under controlled potential and rotation speed. They successfully reduced the concentrations of Cd(II) ions and Cu(II) ions to $< 1.0 \text{ mg L}^{-1}$ from sulphate and chloride media respectively. While selectively removing copper from a mixed Cu/Cd sulphate solution, it was found that Cd(II) concentration did not interfere with the removal of copper at -500 mV vs. SCE. When the potential is switched to -1000 mV vs. SCE, it was possible to reduce the concentration of cadmium to $< 0.5 \text{ mg L}^{-1}$.

Ponde de León and Pletcher (1996) investigated the influence of anions such as Cl^- , NO_3^- , ClO_4^- , BF_4^- and SO_4^{2-} at 298 K on the removal of lead using three grades of RVC (10, 60 and 100 ppi). It was shown that only removal of Pb(II) from chloride medium was under mass transport control. For NO_3^- , ClO_4^- and BF_4^- , the removal of lead to $< 1.0 \text{ mg L}^{-1}$ was possible but the rate was slower than in the chloride medium. Only 20% of lead was removed from sulphate medium after 3000 s of electrolysis. The removal percentage was raised to 90% in 2000-3000 s with an increase of temperature to 333 K. Rodriguez-Valendez *et al.* (2005) had shown that the reduction of Cr(IV) to Cr(III) was viable using RVC electrodes in a parallel flow-